Biochimica et Biophysica Acta 1797 (2010) 143–151

Contents lists available at ScienceDirect

Biochimica et Biophysica Acta

journal homepage: www.elsevier.com/locate/bbabio

Alteration of mitochondrial oxidative phosphorylation in aged skeletal muscle involves modification of adenine nucleotide translocator

Gilles Gouspillou [a], Isabelle Bourdel-Marchasson [a,b], Richard Rouland [a], Guillaume Calmettes [a], Jean-Michel Franconi [a], Véronique Deschodt-Arsac [a], Philippe Diolez [a,*]

[a] Résonance Magnétique des Systèmes Biologiques, UMR 5536 CNRS – Université Victor Segalen Bordeaux 2, 146 rue Léo Saignat, 33076 Bordeaux cedex, France
[b] CHU de Bordeaux, Pôle de gérontologie clinique, Hôpital Xavier Arnozan, 33600 Pessac, France

ARTICLE INFO

Article history:
Received 25 June 2009
Received in revised form 4 September 2009
Accepted 9 September 2009
Available online 12 September 2009

Keywords:
Mitochondrial oxidative phosphorylation
Top-down control analysis
Skeletal muscle
Adenine nucleotide translocator
Aging

ABSTRACT

The process of skeletal muscle aging is characterized by a progressive loss of muscle mass and functionality. The underlying mechanisms are highly complex and remain unclear. This study was designed to further investigate the consequences of aging on mitochondrial oxidative phosphorylation in rat gastrocnemius muscle, by comparing young (6 months) and aged (21 months) rats. Maximal oxidative phosphorylation capacity was clearly reduced in older rats, while mitochondrial efficiency was unaffected. Inner membrane properties were unaffected in aged rats since proton leak kinetics were identical to young rats. Application of top-down control analysis revealed a dysfunction of the phosphorylation module in older rats, responsible for a dysregulation of oxidative phosphorylation under low activities close to in vivo ATP turnover. This dysregulation is responsible for an impaired mitochondrial response toward changes in cellular ATP demand, leading to a decreased membrane potential which may in turn affect ROS production and ion homeostasis. Based on our data, we propose that modification of ANT properties with aging could partly explain these mitochondrial dysfunctions.

1. Introduction

Mitochondria, because of their central role in ATP supply through oxidative phosphorylation, play a crucial role in skeletal muscle function. During last decades, a growing interest has been focused on possible mechanisms linking dysfunctions of the mitochondrial oxidative phosphorylation and the aging process, but implication of oxidative phosphorylation is still a matter of debate. Indeed, mitochondrial oxidation and phosphorylation activities, assessed at rest in vivo by $^{13}C/^{31}P$ NMR spectroscopy, were found to decrease in skeletal muscle of elderly [1]. In accordance with this result, skeletal muscle oxidative capacity, determined using the kinetics of PCr recovery after exercise as an indicator of the maximal rate of oxidative phosphorylation, has been found to decrease with aging in human vastus lateralis [2]. This result was explained by the authors by a concomitant decrease of mitochondrial mass and activity [2]. However, using the same methodology, Kent-Braun and Ng [3] did not find any modification of oxidative capacity with aging in tibialis anterior. In addition, by investigating the effect of aging on ATP producing pathways in vivo in human skeletal muscle, Lanza et al. [4] have found an unaltered oxidative capacity associated with a reduced contribution of glycolysis flux in the ATP turnover during high intensity contraction.

Experiments performed on isolated mitochondria have also brought conflicting results. Reduction of several respiratory chain complexes activities has been reported in several tissues, including skeletal muscle, of aged mice [5]. A decreased maximal oxidation rate during aging was found in skeletal muscle of mice [6], rats [7], and from biopsies of human skeletal muscle [8]. In addition, maximal ATP production was also found to decline with aging in skeletal muscle of rats [9] and humans [10]. However, Rasmussen et al. [11] did not find any modification of mitochondrial oxidative phosphorylation with aging in mitochondria isolated from biopsies of human muscles, and the maximal ADP-stimulated oxidation rate was found to be unaltered in aged rats in several experiments [12,13].

As a consequence, these conflicting results obtained both in vivo and in vitro point out the complexity of the demonstration and the identification of the consequences of aging on mitochondrial oxidative phosphorylation. Moreover, data obtained from in vitro studies are limited to resting (state IV) and maximal (state III) oxidative phosphorylation activities, which are extreme conditions certainly far from in vivo conditions of mitochondrial functioning. Indeed, even though muscle needs very high ATP turnover during maximal contractile activities, muscle activity mainly occurs at moderate activities, corresponding to low ATP turnover and consequently to intermediate mitochondrial activity. Therefore, it appears important to bring information over the whole range of oxidative phosphorylation activity. In addition, the study of the interactions existing between the different components of oxidative phosphorylation is required in

* Corresponding author. Tel.: +33 5 57 57 10 18; fax: +33 5 57 57 45 56.
E-mail address: philippe.diolez@rmsb.u-bordeaux2.fr (P. Diolez).

0005-2728/$ – see front matter © 2009 Elsevier B.V. All rights reserved.
doi:10.1016/j.bbabio.2009.09.004

order to gain a comprehensive overview of the consequences of aging on the integrated functioning of the mitochondrial oxidative phosphorylation.

Top-down control analysis is an efficient approach to study oxidative phosphorylation ranging from state IV to state III. It provides the description of how the different components of oxidative phosphorylation interact through the proton-motive force to meet an ATP demand [14–16]. Previous applications of this approach have, for example, allowed better understanding of the very mechanisms at the origin of dysfunction occurring during hypothermic to normothermic reperfusion in rat liver [17] and the description of the effect of temperature on oxidative phosphorylation [18].

In the present study, we took advantage of the capabilities of the top-down control analysis to carefully investigate possible alterations of oxidative phosphorylation occurring with aging.

2. Materials and methods

2.1. Isolation of skeletal muscle mitochondria

Male Wistar rats aged of 6 and 21 months were anaesthetised with isofluran inhalation and killed by intraperitoneal injection of pentobarbital (60 mg/kg). The two gastrocnemius muscles were then dissected and washed in the isolation medium containing 100 mM sucrose, 180 mM KCl, 50 mM Tris, 5 mM $MgCl_2$, 10 mM EDTA, and 0.1% (wt./vol.) BSA (pH 7.2). Before homogenisation, muscles were minced and exposed during 5 minutes to protease (2 mg of bacterial proteinase type XXIV per ml of isolation medium, Sigma-Aldrich: P8038). Mitochondria were extracted as described in Cannon and Lindberg [19]. All experiments were conducted in agreement with the National and European Research Council Guide for the care and use of laboratory animals. P. Diolez has been attributed a permanent license to conduct experiments on animals by the Service Vétérinaire de la Santé et de la Protection Animale of the Ministère de l'agriculture et de la Forêt (03/17/1999, license number 3308010).

2.2. Protein content determination

Mitochondrial protein concentration was determined by the Bradford method [20] using BSA as standard.

2.3. Simultaneous monitoring of oxidation rate, membrane potential, and phosphorylation rate

Oxygen consumption, membrane potential, and ATP synthesis were monitored simultaneously (cf. Fig. 2) in a glass vessel (final volume 3 ml) in a medium containing 140 mM sucrose, 100 mM KCl, 1 mM EGTA, 20 mM $MgCl_2$, 10 mM KH_2PO_4, and 0.1% (wt./vol.) BSA (pH 7.2). Mitochondrial protein concentration used in the measurement vessel was approximately 0.3 mg ml^{-1} unless for the proton leak flux determination where the protein concentration used was approximately 0.6 mg ml^{-1}. Succinate (5 mM + rotenone 2 μg ml^{-1}) was used as a substrate for the monitoring of oxidative phosphorylation parameters (i.e., oxidation rate, membrane potential, and phosphorylation rate) and top-down control analysis experiments. State III oxidation rates were obtained by adding ADP (250 μM) and state IV oxidation rate was measured after complete ADP phosphorylation.

Oxidation by complex I was evaluated using glutamate (5 mM) + malate (1 mM) or pyruvate (5 mM) + malate (1 mM). State III oxidation rates were obtained using 500 μM ADP. These experiments were carried out in a separate glass vessel in order to avoid any possible residual effect of rotenone on further experiments. To inhibit residual adenylate kinase activity, excess of P1,P5-Di(adenosine-5)pentaphosphate (AP5A, 20 μM) was added to the measurement medium in all experiments. Oxidation rates were determined polarographically with a Clark electrode (Rank Brothers) at 25 °C. Concentration in air-equilibrated medium was taken as 240 μM [18].

Membrane potential was monitored using a homemade tetraphenylphosphonium (TPP^+) electrode coupled to an Ag/AgCl-saturated reference electrode (Tacussel Mi402). Membrane potential ($\Delta\psi$) was calculated by using the Kamo equation [21]:

$$\Delta\psi = \left(\frac{RT}{F}\right) \times \log\left(\frac{v}{V}\right) - \left(\frac{RT}{F}\right) \times \log\left(10^{\frac{\Delta E \times F}{RT}} - 1\right) \quad (1)$$

where v is the mitochondrial matrix volume, V is the volume of measurement medium, and ΔE is the deflection of the TPP^+ electrode from the baseline, derived from the electrode calibration. Mitochondrial matrix volume was taken as 0.79 μl in accordance to Stumpf et al. [22]. To calibrate the TPP^+ electrode response, the TPP^+ concentration in the vessel was doubled (from 1.67 to 3.34 μM) at the beginning of each recording. At the end of each experiment, membrane potential was collapsed by 1 μM carbonyl cyanide *m*-chlorophenylhydrazone (CCCP) to obtain the membrane potential baseline. Due to the lipophilic property of TPP^+, a correcting factor of 50 mV was subtracted from all measurements in order to remove the contribution of the non-specific fixation of TPP^+ in mitochondrial membranes [23] (cf. Fig. 2).

The determination of phosphorylation rate lies on the chemical properties of ATP synthesis reaction. As ATP synthesis is stoichiometrically linked to H^+ consumption (cf. Eq. (2)), the phosphorylation rate was experimentally determined by continuously monitoring the pH variations of the measurement medium [24]. pH changes were converted into rate of H^+ consumption after calculating the buffering capacity determined by successive additions of a titrated HCl solution (0.1 mM) carried out during each assay (cf. Fig. 2). This calibration was also used to ensure that the pH electrode response was never rate limiting. Lastly, rate of H^+ consumption was converted into rate of ATP synthesis by using the following equilibrium [25]:

$$ADP^{q-} + Pi^{r-} + mH^+ \leftrightarrow ATP^{p-} + H_2O \quad (2)$$

with $m = q + r - p$. m corresponds to the number of moles of H^+ required for the synthesis of one mole of ATP mole and depends on the pH and protonation states of ADP, ATP, and Pi. The value of m as a function of pH has been determined by the group of Nishimura [25], and the adequate value has been used to calculate the rate of ATP synthesis in each assay after determination of the actual pH value.

2.4. Top-down control analysis

As previously applied to study the mitochondrial oxidative phosphorylation in mitochondria from different organs [14,17,18,26], oxidative phosphorylation of mitochondria from skeletal muscle was described as three large modules linked by a common thermodynamic intermediate (Fig. 1). In this system, the substrate oxidation module

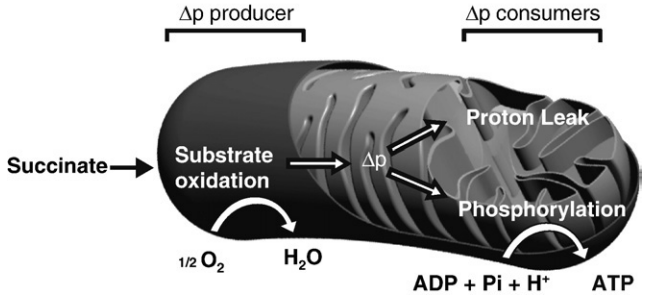

Fig. 1. System definition for top-down control analysis of mitochondrial oxidative phosphorylation. In this system, the mitochondrial functioning is described by three modules, each one grouping several reactions (see Materials and methods for details), connected by a common thermodynamic intermediate (Δp).

(substrate translocases, dehydrogenases, and respiratory chain complexes) generates the proton-motive force (Δp), which is consumed by the phosphorylation module (Pi translocator, ANT, and ATP synthase) to produce ATP and by the proton leak module (passive permeability of the mitochondrial inner membrane to protons and any cation cycling reactions). In the present study, Δp was approximated by the measurement of the membrane potential $\Delta\psi$, which can be considered as a suitable intermediate [27].

The top-down control analysis lies on the experimental determination of the elasticity coefficients over Δp of the three modules. As a consequence, the complete and accurate top-down control analysis of skeletal muscle oxidative phosphorylation requires the experimental determination of the flux through each module and the measurement of intermediate concentration (i.e., the membrane potential value). The fluxes through the substrate oxidation and phosphorylation modules were recorded simultaneously with the membrane potential. The flux of the proton leak module was determined separately during a state IV titration [17,18].

2.5. Modular kinetic analysis and determination of elasticity coefficients over $\Delta\psi$

Elasticity coefficients of each modules can be calculated using modular kinetic analysis [28]. This analysis consists in modifying the value of the intermediate ($\Delta\psi$) by an adequate titration of a module that differs from the module under consideration. To cover the whole range of phosphorylation rates (from state IV to state III), these titrations were performed using succinate as a substrate at different concentrations of atractyloside in presence of excess of ADP [17,18]. Succinate was used as a substrate because it gives a valid picture of how the control is distributed for all substrates [29]. The different module fluxes were measured only when true steady states were reached, i.e., when membrane potential values were constant. The experimental protocol used to determine the kinetic response of each module to membrane potential and the calculation of elasticity coefficients for each module were extensively described [17,18].

2.6. Determination of control coefficients

Overall control coefficients are defined as the fractional change in flux (flux control coefficient) or in $\Delta\psi$ (concentration control coefficients) in response to an infinitesimal change in the activity of the module under consideration. The control coefficients obtained describe a control pattern that gives an overview of the integrated system functioning and of how this system is regulated in response to a change in activity, i.e., a change in cellular ATP demand. Overall flux control coefficients can be calculated from the overall elasticity coefficients by using the equations given in Hafner et al. [14].

However, since phosphorylation rates were experimentally determined in the present study (as nmol ATP min^{-1} mg^{-1}), they were converted into oxygen consumption using the ATP/O ratio determined experimentally for each experiment.

2.7. Statistics

Experimental values are expressed as mean ± SEM for each group of age. Comparisons between young and aged rats were performed using unpaired bilateral Student's *t*-tests. *P*-values were fixed at 0.05 and 0.01 to consider a significant level of difference between series of data.

3. Results

3.1. Morphometric parameters and mitochondrial extraction

Aged rats presented a significantly higher body weight associated with a significantly reduced gastrocnemius weight compared to young rats (Table 1). The sarcopenic index, defined as the gastrocnemius-to-body weight ratio, was significantly lower in the aged group. In contrast to total mitochondrial protein extraction, significantly lower in aged rats, we did not find any modification of the mitochondrial extraction yield, expressed as the amount of mitochondrial protein extracted (in mg) per gram of muscle (Table 1). Consequently, on the basis of this similar extraction yield, the mitochondrial content was unchanged in the gastrocnemius of the 21-month-old rats compared to young rats.

Table 1
Consequences of aging on morphometric parameters and mitochondrial extraction.

	Young ($n=9$)	Aged ($n=10$)
Body weight (g)	561 ± 60	628 ± 32**
Gastrocnemius weight (g)	6.48 ± 0.52	4.78 ± 1.19**
Sarcopenic index (%)	1.16 ± 0.09	0.77 ± 0.20**
Extracted mitochondria (mg)	16.40 ± 2.02	13.58 ± 3.77
Isolation yield (mg of protein/g of muscle)	2.53 ± 0.2	2.86 ± 0.58

Values, obtained from young (6 months) and aged (21 months) rats, are expressed as mean ± SEM. Sarcopenic index correspond to the gastrocnemius weight-to-body weight ratio, expressed as percentage. Differences were tested using an unpaired bilateral Student's *t*-test.
** $p<0.01$ vs. young group.

3.2. Classical parameters of mitochondrial oxidative phosphorylation

The first step of this study was to determine the consequences of aging on the classical parameters of oxidative phosphorylation, i.e., oxygen consumption, phosphorylation rate, and membrane potential. Excess of AP5A was added to the measurement medium in order to avoid any interference in ATP/ADP turnover due to residual activity of adenylate kinase. The assessment of these classical parameters was performed simultaneously using succinate as a substrate. A typical experimental trace recorded using mitochondria isolated from young rats is presented in Fig. 2A. The first step of each experiment was to calibrate the TPP^+-sensitive electrode, performed by adding increasing concentrations of TPP^+. Succinate (5 mM) and a very low amount of ADP (66 μM) were added to the measurement medium just before addition of mitochondria in order to warm-up oxidative phosphorylation and thus prepare mitochondria to subsequent ADP additions. The addition of mitochondria induced a decrease in TPP^+ concentration in the medium, indicating TPP^+ uptake by mitochondria in response to the generation of a transmembrane potential. This generation was due to succinate oxidation, evidenced by the onset of the oxidation rate. Since a small amount of ADP was present during warm-up, phosphorylation stopped rapidly and a steady state was reached, characterized by a high membrane potential value associated with a slow oxidation rate. The following addition of 250 μM ADP was used to obtain state III conditions, where membrane potential was decreased and oxidation rate increased. During state III, pH evolution was measured and used to calculate ATP synthesis rate (see Materials and methods). After ADP was phosphorylated, mitochondria returned to state IV. At the end of each recording, the addition of an uncoupler (CCCP) caused the collapse of the membrane potential and the complete release of TPP^+ from the mitochondria.

Results of these experiments performed on mitochondria from young and aged rats are presented in Table 2. Neither state III nor state IV membrane potential values were modified with aging. However, while state IV oxidation rate was similar between young and aged rats, state III oxidation rate and respiratory control ratio were significantly decreased in aged rats. Phosphorylation rate under state III conditions was also decreased in aged rats. However, the ATP/O ratio was unaffected by aging.

The maximal capacity of respiratory chain was investigated by addition of an uncoupler (CCCP) to collapse the membrane potential and, consequently, to completely release the inhibition exerted by the

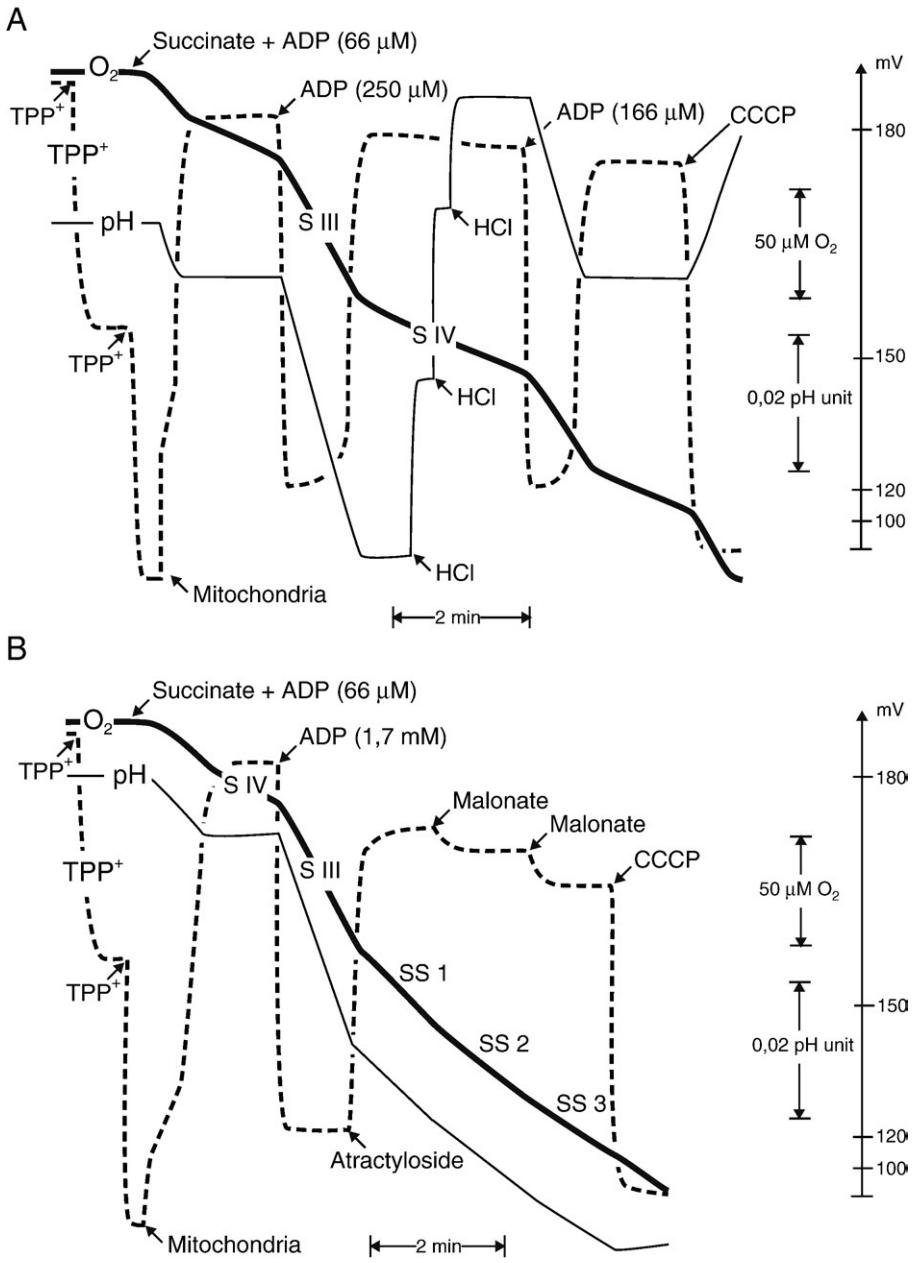

Fig. 2. Simultaneous recording of oxidation rate, membrane potential and phosphorylation rate. (A) Typical recording for determination of classical parameters of oxidative phosphorylation. These recordings were performed using succinate as a substrate (5 mM). Membrane potential was monitored using a TPP^+-sensitive electrode, allowing to follow the TPP^+ concentration in the medium. This electrode was calibrated by two successive additions of 1.67 μM TPP^+. At the end of each experiment, 1 μM CCCP was added to collapse to obtain the membrane potential baseline. Phosphorylation rate was monitored using a pH electrode, calibrated using successive additions of a titrated HCl solution (0.1 mM) (cf. Materials and methods section for details). State III parameters were determined using the addition of 250 μM ADP. State IV parameters were determined after the complete phosphorylation of the added 250 μM ADP (cf. Table 2). (B) Typical recording for determination of the kinetics responses of substrate oxidation and phosphorylation rates modules over the whole range of membrane potential values. Intermediate phosphorylation activities were obtained using variable concentrations of atractyloside, ranging from 0 to 0.9 μM. Actual recording presented here was obtained by adding 0.9 μM atractyloside. S III: state III. S IV: state IV. SS: steady state.

Table 2
Consequences of aging on the classical parameters of mitochondrial oxidative phosphorylation.

	Membrane potential (mV)		Depolarization (mV)	Oxidation rate (nmol O_2 min^{-1} mg^{-1})			RCR	Phosphorylation rate (nmol ATP min^{-1} mg^{-1})	ATP/O ratio
	State IV	State III		State IV	State III	Maximal capacity			
Young ($n=9$)	179.9 ± 4.7	123.9 ± 6.0	56.0 ± 3.9	45.3 ± 2.4	215.5 ± 26.2	217.4 ± 17.4 (n = 5)	4.8 ± 0.6	752.9 ± 80.0	1.75 ± 0.10
Aged ($n=9$)	178.7 ± 3.1	122.3 ± 6.2	56.4 ± 4.8	43.1 ± 4.0	173.7 ± 18.6**	178.8 ± 1.6** (n = 3)	4.0 ± 0.4**	615.4 ± 124.5*	1.76 ± 0.25

Membrane potential value, oxidation rate, and phosphorylation rate were recorded simultaneously in mitochondria oxidizing succinate as a substrate. State III oxidation and phosphorylation rates were obtained by addition of 250 μM ADP. Maximal oxidation rates were obtained using successive additions of CCCP until complete abolishment of the membrane potential. Values are expressed as mean ± SEM. RCR: respiratory control ratio. Differences were tested using an unpaired bilateral Student's *t*-test.

* $p<0.05$ vs. young group.

** $p<0.01$ vs. young group.

Table 3
Consequences of aging on complex I substrates oxidation.

	Young ($n=5$)	Aged ($n=5$)
Glutamate + malate		
State III oxidation rate (nmol O_2 min^{-1} mg^{-1})	343.6 ± 23.5	276.3 ± 26.1**
State IV oxidation rate (nmol O_2 min^{-1} mg^{-1})	16.5 ± 1.1	16.5 ± 1.4
RCR	21.0 ± 2.5	16.9 ± 2.2*
Pyruvate + malate		
State III oxidation rate (nmol O_2 min^{-1} mg^{-1})	271.2 ± 23.8	222.6 ± 24.7*
State IV oxidation rate (nmol O_2 min^{-1} mg^{-1})	15.7 ± 1.1	15.1 ± 0.9
RCR	17.3 ± 1.6	14.8 ± 1.3*

Mitochondrial oxygen consumption was evaluated using glutamate + malate (5 and 1 mM, respectively) or pyruvate + malate (5 and 1 mM, respectively) as substrates. State III oxidation rates were obtained by addition of 500 μM ADP. Values are expressed as mean ± SEM. Differences were tested using an unpaired bilateral Student's *t*-test.
* $p<0.05$ vs. young group.
** $p<0.01$ vs. young group.

proton-motive force on the respiratory chain. Results are presented in Table 2. In addition to the reduced state III oxidation rate, the maximal chain activity was significantly reduced in aged group. Interestingly, the maximal chain activity was very close to the state III oxidation rate for both young and aged rats, indicating that under state III conditions, the activity of the respiratory chain was maximal.

Finally, to complete the assessment of the consequences of aging on classical parameters of oxidative phosphorylation, complex I substrates oxidation was also investigated using glutamate + malate and pyruvate + malate as substrates. Results are presented in Table 3. As for succinate conditions, state IV oxidation rates were similar between the two groups and both state III oxidation rates and respiratory control ratios were also significantly reduced in aged rats. Interestingly, state III oxidation rates were largely higher with substrates of complex I than with succinate. As a consequence, under state III conditions, the phosphorylation capacity largely exceeds the oxidative capacity when succinate is oxidized by these mitochondria.

3.3. Top-down control analysis of oxidative phosphorylation

Top-down control analysis is an integrative approach useful to determine changes that have true functional consequences and is unresponsive to any changes that have no functional consequences [28]. This property has been previously used to determine which module(s) is/are responsible for mitochondrial dysfunctions occurring during physiological [18] or pathophysiological events [17]. Consequently, this approach appears well suited to obtain a precise description of which of the changes occurring during aging have functional consequences for the integrated oxidative phosphorylation.

3.4. Modular kinetics analysis

Modular kinetic analysis is the first part of the top-down control analysis. It consists of monitoring the kinetics of the different modules of oxidative phosphorylation in response to changes in their common intermediate, the membrane potential. Results are presented in Fig. 3. The proton leak flux presents important variation between the state IV and III, and its behaviour is of fundamental importance for the efficiency of oxidative phosphorylation in vivo. It has been well established that this flux is strictly dependent on the value of membrane potential [30]. As a consequence, the study of the relationship existing between membrane potential and the proton leak flux is required to accurately determine the consequences of aging on this module. This relationship was obtained by progressive inhibition of the respiratory chain using malonate under conditions

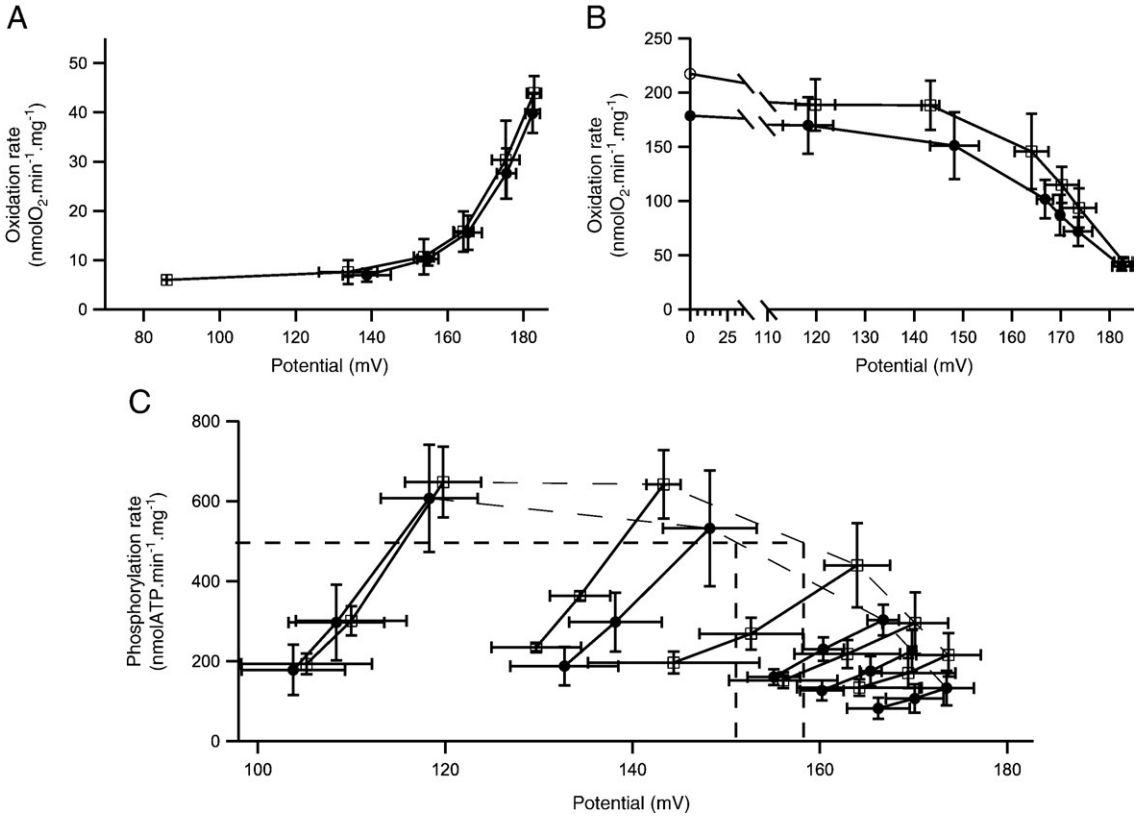

Fig. 3. Modular kinetic analysis of mitochondrial oxidative phosphorylation. Modular kinetic analyses carried out using mitochondria isolated from young (squares) and aged (circles) rats of (A) the proton leak, (B) the substrate oxidation, and (C) the phosphorylation modules. Succinate was used as a substrate. Data of panels B and C are presented as mean ± SEM. Dashed lines illustrate the differences in membrane potential values for young and aged rats corresponding to a given phosphorylation activity.

where proton leakage is the only module that consumes $\Delta\psi$, i.e., in the absence of phosphorylation and/or ATP hydrolysis (excess of oligomycin). Results are presented in Fig. 3A and show that proton leak kinetics was clearly unaffected in the 21-month-old rats.

Kinetic responses of the two other modules, i.e., the substrate oxidation and the phosphorylation modules, were obtained by using specific inhibitor of a module that differ from the module under consideration, in order to modulate the membrane potential value. According to Dufour et al. [18], the kinetic responses of these two modules were determined on the whole range of phosphorylation activities, i.e., from state IV to III, by adding variable concentrations of atractyloside in the presence of an excess of ADP. Fig. 2B shows how these intermediate phosphorylation activities were experimentally obtained on a typical experiment. The onset of the experiment was similar to classical parameters recording. After mitochondria reached state IV, an excess of ADP (1.7 mM final) was added to obtain stable state III conditions. Then atractyloside was added at a concentration ranging from 0 to 0.9 μM in order to set up an intermediate rate of phosphorylation (SS 1) characterized by intermediate values of oxidation rate, phosphorylation rate, and membrane potential. For each atractyloside concentration, SS1 corresponds to the reference steady state. The kinetic response of phosphorylation module to membrane potential—and consequently its elasticity—could then be determined for each atractyloside concentration by successive additions of malonate in order to modulate respiratory chain activity and therefore the membrane potential value. Determination of oxidation rate, phosphorylation rate, and membrane potential was performed after stabilization of membrane potential (see Fig. 2B).

The kinetic responses of the substrate oxidation and phosphorylation modules are presented in Fig. 3B and C, respectively. There was a strong trend for a reduction of both oxidation and phosphorylation rates on the whole range of membrane potential, excepted for the oxidation rate under state IV conditions (no phosphorylation). These results demonstrate a decrease of the activity of mitochondrial oxidative phosphorylation for any given membrane potential value. Moreover, as represented by the dashed lines in Fig. 3C, for the same absolute phosphorylation rate, and by extension for the same cellular ATP demand, membrane potential was clearly lower in mitochondria isolated from aged rats.

Fig. 4 presents the results of the titration of the phosphorylation module obtained by adding variable concentrations of atractyloside. This titration, initially performed to determine the kinetic response of the substrate oxidation module, has revealed that mitochondria isolated from aged muscles were significantly more sensitive to atractyloside than young mitochondria (Fig. 4A). This result was confirmed by the calculation of IC_{50} of atractyloside, significantly lowered by about 30% in mitochondria isolated from aged muscles (Fig. 4B).

3.5. Elasticity coefficients

As described in the experimental section, elasticity coefficients for each module were calculated from the data obtained by the modular kinetic analysis. Elasticity coefficients of the three modules, for membrane potential values ranging from state IV to state III, are presented in Fig. 5. The elasticity of the proton leak module was unchanged with aging (Fig. 5A). Similarly, no clear modification of the elasticity of the substrate oxidation module was observed (Fig. 5B). Both in young and old rat mitochondria, the elasticity of substrate oxidation increased rapidly (in absolute value) with membrane potential value, from values close to zero under low membrane potential (high phosphorylation activity, state III) to about −20 at

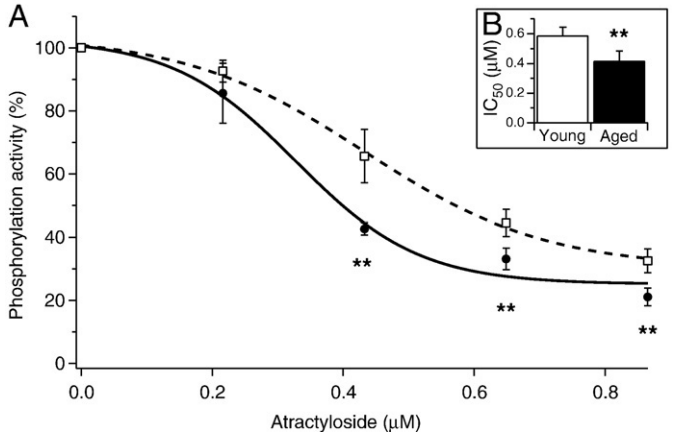

Fig. 4. Influence of aging on the atractyloside-induced inhibition of the phosphorylation rate. (A) Inhibition of the phosphorylation activity obtained by adding increasing atractyloside concentration for young (squares) and aged (circles) rats. For each measurement, ADP (1.7 mM) was present in excess and succinate was used as a substrate. The maximal phosphorylation activity (100%) was determined for each experiment before addition of atractyloside. Dashed and plain curves represent sigmoid fits of data obtained for young and aged rats, respectively. (B) Determination of the half maximal inhibitory concentration (IC_{50}) of atractyloside on young and aged mitochondria. IC_{50} values were determined using sigmoid fits of data obtained for each experiment. $^{**}p<0.01$ between young ($n=6$) and aged groups ($n=7$).

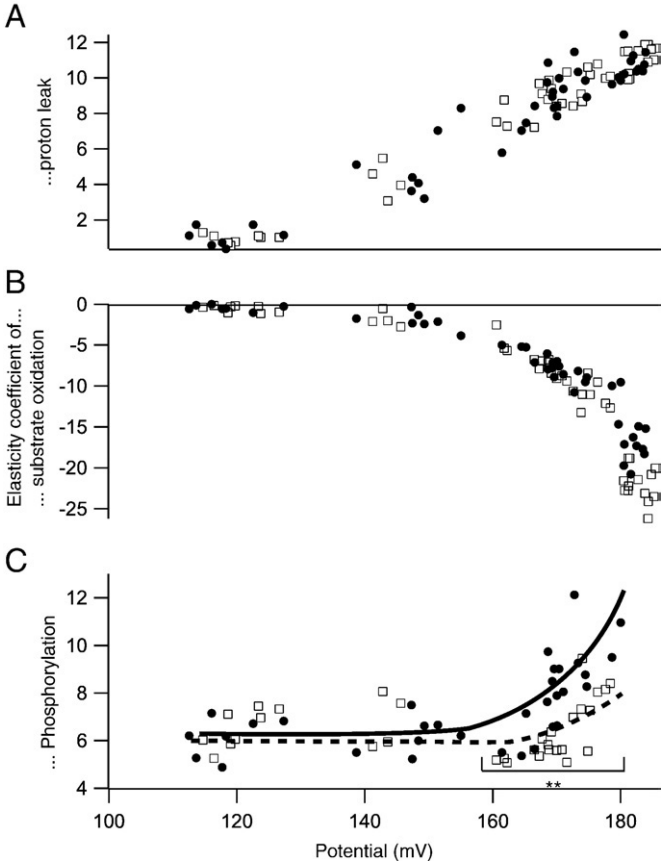

Fig. 5. Influence of aging on elasticity coefficients. Elasticity coefficients of (A) proton leak, (B) substrate oxidation, and (C) phosphorylation modules toward membrane potential for young (squares) and aged (circles) rats. Each measurement was performed using succinate as a substrate (5 mM) and excess of ADP (1.7 mM). Intermediate phosphorylation activities were obtained using variable concentration of atractyloside (cf. Fig. 2). For the phosphorylation module, differences were tested using an unpaired bilateral Student's *t*-test with the average value of elasticity coefficients, for each group, between 160 and 181 mV. $^{**}p<0.01$ between young ($n=7$) and aged groups ($n=7$). Art drawing has been added to emphasize the difference between young and aged rats.

high membrane potential (low phosphorylation activity, approaching state IV).

The same pattern was found for the elasticity curve of phosphorylation module, but with a much smaller increase for high membrane potential values (Fig. 5C). However, this elasticity pattern was significantly modified in mitochondria from aged rats. As compared to young rats, this elasticity was significantly increased for the 21-month-old rats under membrane potential values ranging from 160 to 180 mV (Fig. 5C). It is important to note that this range of membrane potentials corresponds to intermediate phosphorylation activities.

3.6. Control coefficients

Elasticity coefficients were then used to calculate the overall control coefficients of the three modules over each flux and over $\Delta\psi$ as a function of the phosphorylation activity. Control exerted by the different modules over $\Delta\psi$ and over proton leak flux was unchanged with aging (data not shown). As a consequence, only the control coefficients exerted by the three modules over the substrate oxidation and phosphorylation fluxes are presented in Fig. 6. A similar control pattern under high phosphorylation activities was observed between young and aged rats, reflecting the almost identical elasticities under these conditions (low membrane potential). Under these high phosphorylation activities, most of the control is exerted by the substrate oxidation module. As discussed above, this result may be correlated to the observation that, in the presence of succinate, respiratory chain activity is close to maximal activity and therefore exhibits very low elasticity values. By contrast, aged rats presented a significantly modified control pattern of oxidative phosphorylation under intermediate and low phosphorylation activities (i.e., below 50% of the maximal activity). This modified control pattern in aged rats was characterized by an increase of the control exerted by the

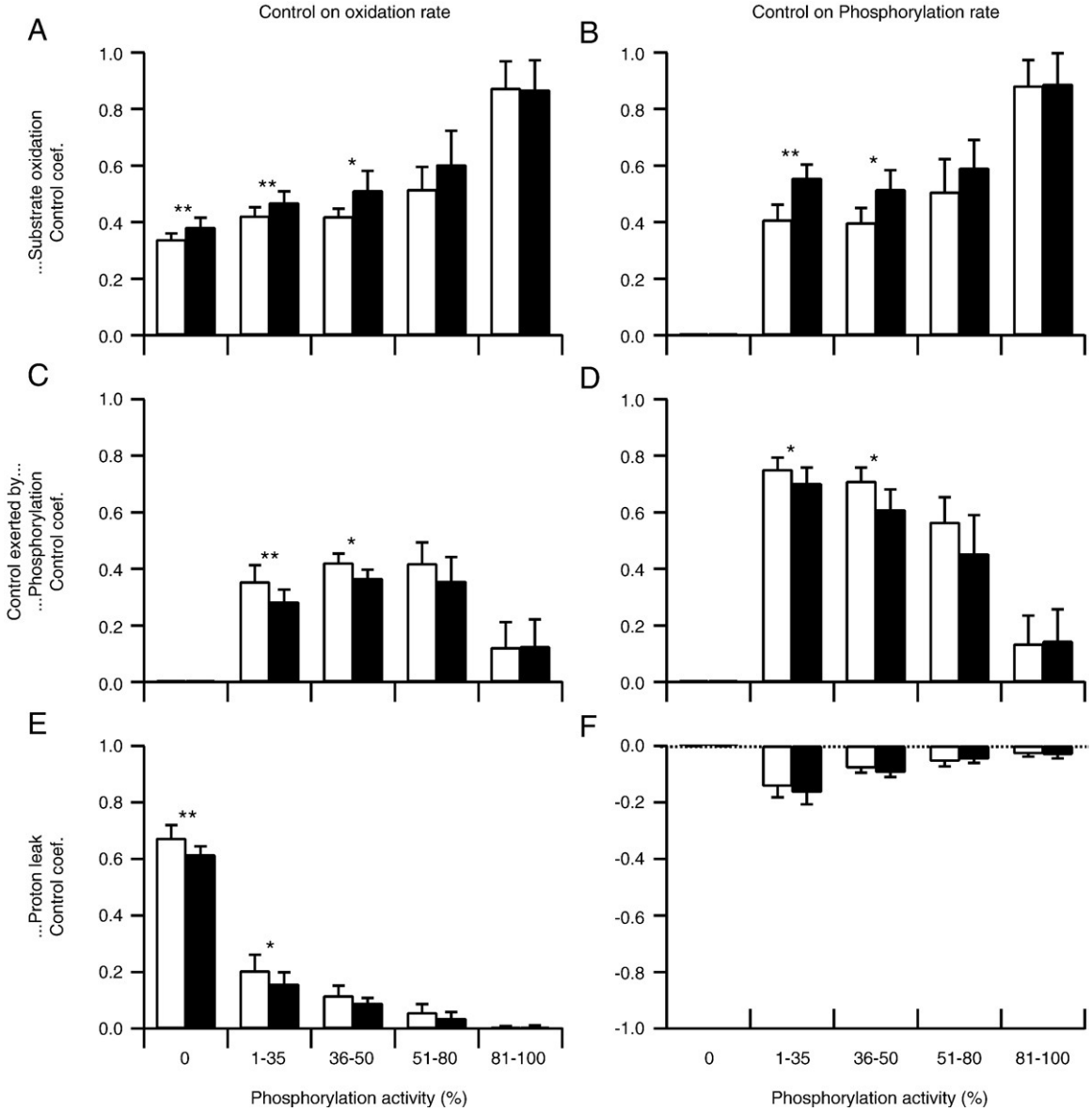

Fig. 6. Influence of aging on the control pattern of oxidative phosphorylation. Control exerted by substrate oxidation (first row), phosphorylation (second row), and proton leak (third row) over oxidation (left column) and phosphorylation rates (right column), for young (open bars) and aged rats (solid bars). Each measurement was performed using succinate as a substrate (5 mM) and excess of ADP (1.7 mM). Intermediate phosphorylation activities were obtained using variable concentration of atractyloside (cf. Fig. 2). For statistical purpose, control coefficients for each population were grouped into different ranges of phosphorylation activity (i.e., 0%, 1% to 35%, 35% to 50%, 50% to 80%, and 80% to 100% of the maximal phosphorylation rate). The maximal phosphorylation activity (100%) was determined for each experiment during the determination of the state III elasticity coefficients of the top-down control analysis. Values are presented as mean ± SEM. Differences were tested using an unpaired bilateral Student's *t*-test. $^{**}p<0.01$, $^{*}p<0.05$ between young ($n=7$) and aged groups ($n=7$).

substrate oxidation module (Fig. 6A and B) and a concomitant decrease of the control exerted by the phosphorylation module over both the substrate oxidation and phosphorylation module fluxes (Fig. 6C and D), which are the direct consequence of the increase in the elasticity of the phosphorylation (see Fig. 5C) and summation theorem. In other words, in the absence of change in substrate oxidation and leak elasticities at high membrane potential (Fig. 5A and B), the increase in elasticity of phosphorylation module in aged rat mitochondria is responsible for a decreased control by this latter module and, the sum of the control being 1, control by substrate oxidation increases.

4. Discussion

The present study was designed to investigate the consequences of aging on oxidative phosphorylation in mitochondria isolated from rat skeletal muscle. The gastrocnemius muscle was chosen because of the physiological relevance of the alteration induced by aging, since it is known to be sensitive to sarcopenia [31]. Indeed, this muscle is partly composed of glycolytic fibers, well known to be affected during aging [32]. This sensitivity was confirmed in the present study by the calculation of the sarcopenic index (Table 1), significantly reduced in the 21-month-old rats. Both of the observed changes, increase in body weight and decrease in gastrocnemius weight of these old rats, were similar to those observed in older humans [33].

A current theory to explain skeletal muscle aging is based on the accumulation of oxidative damages to mitochondrial DNA and proteins, due to mitochondrial ROS overproduction (for reviews, see [34,35]). The interest on the properties of the inner mitochondrial membrane is increasing, since it has been proposed that an increased conductance to proton may reduce the ROS production [36]. In this context, the increased proton leak found with aging in studies performed on rat [7] and human muscles [8] has been interpreted as a compensatory mechanism to decrease ROS production. This hypothesis could not be confirmed in the present study, since we provide experimental evidences that the proton leak kinetics and, consequently, the inner membrane properties were unaltered in the 21-month-old rats (Fig. 2A). Moreover, these unaltered properties explain why the mitochondrial efficiency (ATP/O ratio) and membrane potential values under states III and IV were found unchanged with aging (Table 2). However, this study was focused on “middle-aged” rats, and we cannot totally exclude that alterations of inner membrane properties could emerge at advanced stages of aging. Indeed, by studying the effect of aging and caloric restriction on the proton leak kinetics, Asami et al. [37] have proposed that an increase in proton leak may only occur within a brief time span at advanced age.

The study of the classical parameters of oxidative phosphorylation revealed a clear reduction of the maximal capacity of oxidative phosphorylation in aged rats whatever the pathway of electron through the respiratory chain (Tables 2 and 3). This result is in accordance with a previous work of Drew et al. [9], which have reported a decreased maximal phosphorylation rate in mitochondria isolated from rat gastrocnemius muscle with aging. However, the physiological consequences of this reduced maximal capacity of ATP production are difficult to determine, since under usual in vivo conditions, mitochondrial oxidative phosphorylation operates below maximal rates.

To get better insights concerning the consequences of aging on mitochondrial function, we studied the oxidative phosphorylation over the whole range of mitochondrial activities using the top-down control analysis. This approach was also used because it gives an overview of the functioning of the integrated system and has been shown to accurately detect dysfunctions of oxidative phosphorylation [15,17,18,38–41]. Modular kinetic analysis (the first part of the top-down control analysis) revealed that the reduction of both oxidation and phosphorylation rates is not restricted to the maximal activity but is present over the whole range of membrane potentials, i.e., from state IV to III (Fig. 3B and C). The direct consequence of this modified kinetics is that for any cellular ATP demand (an example is shown in Fig. 3C), oxidative phosphorylation activity occurs at a lower membrane potential in aged rats compared to young rats. This lower membrane potential value for any requested cellular ATP demand may have important consequences on cellular energetics. Indeed, it is now clearly established that mitochondria play an important role in the cellular calcium homeostasis. Calcium entry into the mitochondrial matrix, as for other ions, is in part function of the membrane potential (for review, see [42]). A lower membrane potential for the same relative cellular ATP demand (same metabolic state) would induce a lower sequestration of calcium by the mitochondria. Interestingly, the resting calcium concentration was found to increase with aging in several rats muscles [43] and the calcium-dependent proteolytic system has been implicated in the loss of muscle mass occurring with aging [44]. As a consequence, on the basis of our results, we can hypothesize that oxidative phosphorylation dysfunctions induced by aging may take part into mechanisms responsible for the disturbed calcium homeostasis documented with aging. In addition, a lower membrane potential for an equivalent cellular ATP demand may represent a compensatory mechanism to reduce the ROS production, and in turn ROS-induced damages, since ROS production has been demonstrated to show a steep dependence on the magnitude of the proton-motive force [36].

The complete top-down control analysis also revealed an abnormal control pattern of oxidative phosphorylation under weak and intermediate phosphorylation activities in aged rats (Fig. 6). Interestingly this alteration of the internal regulation of the mitochondrial oxidative phosphorylation appears physiologically relevant, since under usual in vivo conditions, and especially at rest and during moderate activities, the cellular ATP demand corresponds to weak phosphorylation activities. This dysregulation is entirely explained by the dysfunction of the phosphorylation module described here since it is the only module whose elasticity was modified under high membrane potential values in aged rats (Fig. 5C). The resulting decrease of the control exerted by this module over the oxidation rate may lead to a lower and inadequate response of the entire oxidative phosphorylation to increased cellular ATP demand. Consequently we can hypothesis that this dysregulation of the integrative functioning, combined with the lower membrane potential value for any cellular ATP demand, can in part explain the decreased ATP content previously reported in the gastrocnemius of aged rats [9]. This decrease in ATP content probably modifies the AMP to ATP ratio, and in turn may disturb the functioning of signaling pathways like the S6K/mTOR/AMPK system involved in the control of muscle mass [45].

Several hypotheses can be put forward to explain the dysfunction of the phosphorylation module observed in the present study. However, the increased sensitivity of mitochondria isolated from aged muscles to atractyloside (Fig. 4) strongly suggests the implication of the adenine nucleotide translocator (ANT). Indeed, ANT is an important component of the phosphorylation module and was shown to be oxidatively modified during aging in the flight muscle of housefly [46] and in rat skeletal muscles [47]. These oxidatively mediated damages, by increasing the ANT carbonyl content and decreasing the ANT functionality [46], may be responsible for the modification of the kinetic properties of the phosphorylation module. An other possible implication of ANT could arise trough its role in the mitochondrial permeability transition pore (mPTP) functioning. Indeed, ANT is considered as an important component of the mPTP [48]. Thiol modification of ANT by oxidative stress has been implicated in mPTP opening (for review, see [49,50]) and we previously demonstrated that mPTP opening disturbs the internal regulation of oxidative phosphorylation [17].

In conclusion, this paper presents the evidence for deleterious alterations of oxidative phosphorylation in the skeletal muscle of aged

rats. Application of the top-down control analysis revealed that alterations of oxidative phosphorylation mainly arise from the phosphorylation module. These alterations are of major interest since they occur at phosphorylation activities compatible with in vivo conditions of mitochondrial functioning in the elderly. While the very mechanisms still need to be thoroughly investigated, we provide in the present study evidence that these dysfunctions involve modification of ANT properties. Further experiments are now required to determine the precise implication of this translocator in the phosphorylation module response to cellular ATP demand. In light of our results, dysfunctions of oxidative phosphorylation induced by aging certainly modify the cellular energetics and physiology by affecting the ROS production and calcium homeostasis.

Acknowledgment

The authors acknowledge Yannick Chatenet for drawing.

References

[1] K.F. Petersen, D. Befroy, S. Dufour, J. Dziura, C. Ariyan, D.L. Rothman, L. DiPietro, G.W. Cline, G.I. Shulman, Mitochondrial dysfunction in the elderly: possible role in insulin resistance, Science 300 (2003) 1140–1142.
[2] K.E. Conley, S.A. Jubrias, P.C. Esselman, Oxidative capacity and ageing in human muscle, J. Physiol. 526 (Pt 1) (2000) 203–210.
[3] J.A. Kent-Braun, A.V. Ng, Skeletal muscle oxidative capacity in young and older women and men, J. Appl. Physiol. 89 (2000) 1072–1078.
[4] I.R. Lanza, D.E. Befroy, J.A. Kent-Braun, Age-related changes in ATP-producing pathways in human skeletal muscle in vivo, J. Appl. Physiol. 99 (2005) 1736–1744.
[5] L.K. Kwong, R.S. Sohal, Age-related changes in activities of mitochondrial electron transport complexes in various tissues of the mouse, Arch. Biochem. Biophys. 373 (2000) 16–22.
[6] A. Mansouri, F.L. Muller, Y. Liu, R. Ng, J. Faulkner, M. Hamilton, A. Richardson, T.T. Huang, C.J. Epstein, H. Van Remmen, Alterations in mitochondrial function, hydrogen peroxide release and oxidative damage in mouse hind-limb skeletal muscle during aging, Mech. Ageing. Dev. 127 (2006) 298–306.
[7] S. Kumaran, K.S. Panneerselvam, S. Shila, K. Sivarajan, C. Panneerselvam, Age-associated deficit of mitochondrial oxidative phosphorylation in skeletal muscle: role of carnitine and lipoic acid, Mol. Cell. Biochem. 280 (2005) 83–89.
[8] M. Tonkonogi, M. Fernstrom, B. Walsh, L.L. Ji, O. Rooyackers, F. Hammarqvist, J. Wernerman, K. Sahlin, Reduced oxidative power but unchanged antioxidative capacity in skeletal muscle from aged humans, Pflugers Arch. 446 (2003) 261–269.
[9] B. Drew, S. Phaneuf, A. Dirks, C. Selman, R. Gredilla, A. Lezza, G. Barja, C. Leeuwenburgh, Effects of aging and caloric restriction on mitochondrial energy production in gastrocnemius muscle and heart, Am. J. Physiol., Regul. Integr. Comp. Physiol. 284 (2003) R474–480.
[10] K.R. Short, M.L. Bigelow, J. Kahl, R. Singh, J. Coenen-Schimke, S. Raghavakaimal, K.S. Nair, Decline in skeletal muscle mitochondrial function with aging in humans, Proc. Natl. Acad. Sci. U. S. A. 102 (2005) 5618–5623.
[11] U.F. Rasmussen, P. Krustrup, M. Kjaer, H.N. Rasmussen, Experimental evidence against the mitochondrial theory of aging. A study of isolated human skeletal muscle mitochondria, Exp. Gerontol. 38 (2003) 877–886.
[12] B. Chabi, V. Ljubicic, K.J. Menzies, J.H. Huang, A. Saleem, D.A. Hood, Mitochondrial function and apoptotic susceptibility in aging skeletal muscle, Aging Cell 7 (2008) 2–12.
[13] J. Kerner, P.J. Turkaly, P.E. Minkler, C.L. Hoppel, Aging skeletal muscle mitochondria in the rat: decreased uncoupling protein-3 content, Am. J. Physiol. Endocrinol. Metab. 281 (2001) E1054–E1062.
[14] R.P. Hafner, G.C. Brown, M.D. Brand, Analysis of the control of respiration rate, phosphorylation rate, proton leak rate and protonmotive force in isolated mitochondria using the 'top-down' approach of metabolic control theory, Eur. J. Biochem. 188 (1990) 313–319.
[15] P. Diolez, A. Kesseler, F. Haraux, M. Valerio, K. Brinkmann, M.D. Brand, Regulation of oxidative phosphorylation in plant mitochondria, Biochem. Soc. Trans. 21 (Pt 3) (1993) 769–773.
[16] G.C. Brown, R.P. Hafner, M.D. Brand, A 'top-down' approach to the determination of control coefficients in metabolic control theory, Eur. J. Biochem. 188 (1990) 321–325.
[17] N. Leducq, M.C. Delmas-Beauvieux, I. Bourdel-Marchasson, S. Dufour, J.L. Gallis, P. Canioni, P. Diolez, Mitochondrial permeability transition during hypothermic to normothermic reperfusion in rat liver demonstrated by the protective effect of cyclosporin A, Biochem. J. 336 (Pt 2) (1998) 501–506.
[18] S. Dufour, N. Rousse, P. Canioni, P. Diolez, Top-down control analysis of temperature effect on oxidative phosphorylation, Biochem. J. 314 (Pt 3) (1996) 743–751.
[19] B. Cannon, O. Lindberg, Mitochondria from brown adipose tissue: isolation and properties, Methods Enzymol. 55 (1979) 65–78.
[20] M.M. Bradford, A rapid and sensitive method for the quantitation of microgram quantities of protein utilizing the principle of protein–dye binding, Anal. Biochem. 72 (1976) 248–254.
[21] N. Kamo, M. Muratsugu, R. Hongoh, Y. Kobatake, Membrane potential of mitochondria measured with an electrode sensitive to tetraphenyl phosphonium and relationship between proton electrochemical potential and phosphorylation potential in steady state, J. Membr. Biol. 49 (1979) 105–121.
[22] D.A. Stumpf, R. Haas, L.A. Eguren, J.K. Parks, R.E. Eilert, Protonmotive force in muscle mitochondria, Muscle Nerve 5 (1982) 14–19.
[23] M. Goubern, J. Yazbeck, M.F. Chapey, P. Diolez, F. Moreau, Variations in energization parameters and proton conductance induced by cold adaptation and essential fatty acid deficiency in mitochondria of brown adipose tissue in the rat, Biochim. Biophys. Acta 1015 (1990) 334–340.
[24] M. Valerio, P. Diolez, F. Haraux, Deactivation of F0F1 ATPase in intact plant mitochondria. Effect of pH and inhibitors, Eur. J. Biochem. 221 (1994) 1071–1078.
[25] M. Nishimura, T. Ito, B. Chance, Studies on bacterial photophosphorylation. III. A sensitive and rapid method of determination of photophosphorylation, Biochim. Biophys. Acta 59 (1962) 177–182.
[26] N.I. Kavanagh, E.K. Ainscow, M.D. Brand, Calcium regulation of oxidative phosphorylation in rat skeletal muscle mitochondria, Biochim. Biophys. Acta 1457 (2000) 57–70.
[27] M.D. Brand, L.F. Chien, D.F. Rolfe, Control of oxidative phosphorylation in liver mitochondria and hepatocytes, Biochem. Soc. Trans. 21 (Pt 3) (1993) 757–762.
[28] T. Amo, M.D. Brand, Were inefficient mitochondrial haplogroups selected during migrations of modern humans? A test using modular kinetic analysis of coupling in mitochondria from cybrid cell lines, Biochem. J. 404 (2007) 345–351.
[29] M.D. Brand, M.E. Harper, H.C. Taylor, Control of the effective P/O ratio of oxidative phosphorylation in liver mitochondria and hepatocytes, Biochem. J. 291 (Pt 3) (1993) 739–748.
[30] M.D. Brand, L.F. Chien, P. Diolez, Experimental discrimination between proton leak and redox slip during mitochondrial electron transport, Biochem. J. 297 (Pt 1) (1994) 27–29.
[31] C. Martin, H. Dubouchaud, L. Mosoni, J.M. Chardigny, A. Oudot, E. Fontaine, C. Vergely, C. Keriel, L. Rochette, X. Leverve, L. Demaison, Abnormalities of mitochondrial functioning can partly explain the metabolic disorders encountered in sarcopenic gastrocnemius, Aging Cell 6 (2007) 165–177.
[32] J. Lexell, Human aging, muscle mass, and fiber type composition, J. Gerontol. A., Biol. Sci. Med. Sci. 50 (Spec No) (1995) 11–16.
[33] F. Fantin, V. Di Francesco, G. Fontana, A. Zivelonghi, L. Bissoli, E. Zoico, A. Rossi, R. Micciolo, O. Bosello, M. Zamboni, Longitudinal body composition changes in old men and women: interrelationships with worsening disability, J. Gerontol. A., Biol. Sci. Med. Sci. 62 (2007) 1375–1381.
[34] A.J. Dirks, T. Hofer, E. Marzetti, M. Pahor, C. Leeuwenburgh, Mitochondrial DNA mutations, energy metabolism and apoptosis in aging muscle, Ageing Res. Rev. 5 (2006) 179–195.
[35] E.J. Lesnefsky, C.L. Hoppel, Oxidative phosphorylation and aging, Ageing Res. Rev. 5 (2006) 402–433.
[36] M.D. Brand, Uncoupling to survive? The role of mitochondrial inefficiency in ageing, Exp. Gerontol. 35 (2000) 811–820.
[37] D.K. Asami, R.B. McDonald, K. Hagopian, B.A. Horwitz, D. Warman, A. Hsiao, C. Warden, J.J. Ramsey, Effect of aging, caloric restriction, and uncoupling protein 3 (UCP3) on mitochondrial proton leak in mice, Exp. Gerontol. 43 (2008) 1069–1076.
[38] A. Kesseler, M.D. Brand, Quantitative determination of the regulation of oxidative phosphorylation by cadmium in potato tuber mitochondria, Eur. J. Biochem. 225 (1994) 923–935.
[39] A. Kesseler, M.D. Brand, Effects of cadmium on the control and internal regulation of oxidative phosphorylation in potato tuber mitochondria, Eur. J. Biochem. 225 (1994) 907–922.
[40] A. Kesseler, M.D. Brand, Localisation of the sites of action of cadmium on oxidative phosphorylation in potato tuber mitochondria using top-down elasticity analysis, Eur. J. Biochem. 225 (1994) 897–906.
[41] A. Kesseler, P. Diolez, K. Brinkmann, M.D. Brand, Characterisation of the control of respiration in potato tuber mitochondria using the top-down approach of metabolic control analysis, Eur. J. Biochem. 210 (1992) 775–784.
[42] B. O'Rourke, Mitochondrial ion channels, Annu. Rev. Physiol. 69 (2007) 19–49.
[43] B. Fraysse, J.F. Desaphy, J.F. Rolland, S. Pierno, A. Liantonio, V. Giannuzzi, C. Camerino, M.P. Didonna, D. Cocchi, A. De Luca, D. Conte Camerino, Fiber type-related changes in rat skeletal muscle calcium homeostasis during aging and restoration by growth hormone, Neurobiol. Dis. 21 (2006) 372–380.
[44] E. Dargelos, C. Brule, L. Combaret, A. Hadj-Sassi, S. Dulong, S. Poussard, P. Cottin, Involvement of the calcium-dependent proteolytic system in skeletal muscle aging, Exp. Gerontol. 42 (2007) 1088–1098.
[45] V. Aguilar, S. Alliouachene, A. Sotiropoulos, A. Sobering, Y. Athea, F. Djouadi, S. Miraux, E. Thiaudiere, M. Foretz, B. Viollet, P. Diolez, J. Bastin, P. Benit, P. Rustin, D. Carling, M. Sandri, R. Ventura-Clapier, M. Pende, S6 kinase deletion suppresses muscle growth adaptations to nutrient availability by activating AMP kinase, Cell Metab. 5 (2007) 476–487.
[46] L.J. Yan, R.S. Sohal, Mitochondrial adenine nucleotide translocase is modified oxidatively during aging, Proc. Natl. Acad Sci. U. S. A. 95 (1998) 12896–12901.
[47] J. Feng, H. Xie, D.L. Meany, L.V. Thompson, E.A. Arriaga, T.J. Griffin, Quantitative proteomic profiling of muscle type-dependent and age-dependent protein carbonylation in rat skeletal muscle mitochondria, J. Gerontol. A., Biol. Sci. Med. Sci. 63 (2008) 1137–1152.
[48] A.P. Halestrap, What is the mitochondrial permeability transition pore? J. Mol. Cell. Cardiol. 46 (2009) 821–831.
[49] A.P. Halestrap, G.P. McStay, S.J. Clarke, The permeability transition pore complex: another view, Biochimie 84 (2002) 153–166.
[50] A.P. Halestrap, C. Brennerb, The adenine nucleotide translocase: a central component of the mitochondrial permeability transition pore and key player in cell death, Curr. Med. Chem. 10 (2003) 1507–1525.